RSC Advances

ROYAL SOCIETY OF CHEMISTRY

www.rsc.org/advances

Calcium alginate microfibers with spindle-knots are fabricated by using a microfluidic and wet-spinning technique. The fabrication process is investigated in detail, considering factors like the two-phase flow rate ratio, the micropipette diameter, and viscosity of organics. This fabrication process is simple and controllable, and the ability to collect water of fibers makes it possible to develop further applications.

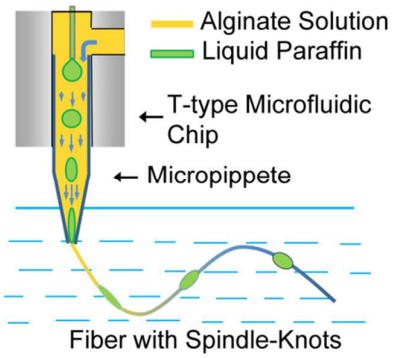

Journal Name

RSCPublishing

ARTICLE

Continuous generation of alginate microfibers with spindle-knots by using a simple microfluidic device

Cite this: DOI: 10.1039/xoxxoooooox

Xiaobo Ji,[a] Song Guo,[a] Changfeng Zeng,[b] Chongqing Wang[a] and Lixiong Zhang*[a],

Received ooth January 2012,
Accepted ooth January 2012

DOI: 10.1039/xoxxoooooox

www.rsc.org/

We develop a simple microfluidic-based method to fabricate calcium alginate microfibers with spindle-knots. A co-axial type microfluidic device installed with a micropipette at its outlet is used with the sodium alginate solution as the continuous phase and liquid paraffin as the dispersed phase. We examine the effect of the micropipette, its diameter, the dispersed phase to the continuous phase flow rate ratio and the physical properties of the oil used as the dispersed phase on the formation of the knots, the width and height of the knot, the interval between two adjacent knots, and the diameter of the fiber. Use of the micropipette is crucial to successful formation of the knots, as the oil phase microdroplets are deformed when flowing through it and retract after flowing out of it. The height and width of the knot increase and the interval decreases with increasing the flow rate ratio and the microdroplet diameter. The viscosity of the oil phase plays an important role in successful formation of the knots. The alginate fibers with spindle-knots exhibit water collection capability. This method is expected to be used for fabrication of other types of fibers with spindle-knots.

Introduction

Submillimetric artificial fibers have attracted much attention because of their analog to the fibers found in nature and broad application in the field of tissue engineering, drug discovery, and biotechnology.[1-4] They are mostly cylindrical in shape[5], as well as fibers with flat[6], flat with groove[7] and asymmetric shapes[8] are also reported. Recently, a new kind biomimetic fiber inspired by spider silk with special periodic spindle-knots structure has gained some concerns owing to its unique wettability, and have been applied in tissue engineering and drug delivery. [4,9] Several methods have been developed to fabricate these biomimic fibers, including dip-coating, fluid-coating, and electrodynamic technology.[10] The dip-coating method is conducted by immersing a nylon fiber into a poly(vinyl acetate), poly(methyl methacrylate) (PMMA), poly-styrene (PS), or poly(vinylidene fluoride) solution, followed by drawing out. Polymer droplets are thus formed on the nylon fiber, which later become periodic spindle-knots after solvent evaporation.[11] The fluid-coating method is designed to continuously draw a nylon fiber horizontally through a reservoir of the above polymer solution from a capillary tube attached horizontally to the reservoir wall.[12] The electrodynamic technology, based on the electrospinning and electrospraying technique, is carried out by coaxial jetting of poly(ethylene glycol) in DMF (dimethyl formamide) and methylene chloride as the outer fluid and PS in DMF as the inner fluid in an electric field.[13] All the three methods are based on the Rayleigh instability that the polymer film formed on the fibers would break up into polymer droplets.[14] Thus, there exist difficulties in fine control of the size of the knots and the interval between two adjacent knots. Furthermore, the fibers are different from the spindle-knots in term of the materials made of them.

In 2011, Kang et al. proposed a microfluidic technique for fabrication of calcium alginate fibers with spindle-knots by using a microfluidic chip combined with a digital fluid controller and pneumatic valves system.[15] Two alternating sodium alginate fluid streams are introduced into a microchannel by the valves so that evenly spaced spindle-knots are formed. Although this technique is versatile to control topography and structure of the fiber, complex digital fluid controller and pneumatic valves have to be used and the obtained structured fiber is all constructed by calcium alginate. Herein, we propose a simple method based on the microfluidic technique and wet-spinning process to fabricate calcium alginate fibers with spindle-knots in which other component is introduced. The formation principle rests upon the deformation and retraction dynamics of drops under extensional flow.[16,17] We only use a simple co-axial type microfluidic chip to generate oil phase microdroplets in sodium alginate continuous phase and a micropipette installed at the outlet of the chip to deform the microdroplets. Thus, spindle-knots containing oil phase microdroplets are formed on the resultant calcium

alginate fiber by the supporting effect of internal organics and chelation of the Ca^{2+}. These fibers with spindle-knots also exhibit the water collection capability, same as those of the fibers with similar structure prepared by the above mentioned methods. The novelty of this fabrication process lies on its simplification of the microfluidic device and controllability of the fibers' structure. Furthermore, the alginate fiber with spindle-knots may have potential new applications in the fields of filtration and sensing.

Experimental Section

Materials. Sodium alginate, sodium dodecyl sulfate (SDS) and n-hexadecane were purchased from Sinopharm Chemical Reagent Co., Ltd. Sudan III, dimethylsilicone oil DC-200/10, DC-200/50 and DC-200/100 were purchased from Aladdin Reagents (Shanghai) Co., Ltd. Liquid paraffin, 1,2-dichloroethane, n-heptane, o-xylene, 1-octanol liquid and oleic acid were purchased from Shanghai Lingfeng Chemical Reagent Co., Ltd. The interfacial tension and the viscosity were, respectively, measured by drop weight technique and Ostwald's viscometer at 25 °C.

Fabrication of fibers with spindle-knots. Preparation of calcium alginate fibers was carried out in a co-axial type microfluidic device with a sodium alginate solution as the continuous phase and the liquid paraffin as the dispersed phase. The co-axial type microfluidic device was fabricated on two PMMA plates by carving two perpendicular microchannels with their width of 1 mm and depth of 0.5 mm to form a T-shaped channel chip using an engraving machine (MDX-40A, Roland). A metal needle (inner diameter = 0.11 mm) was inserted into the T-shaped chip from the top side, and a micropipette was also inserted into the same channel from the other end. The tip of the needle was co-axially inserted into the micropipette. The inlet of the micropipette was positioned just at the downstream of the outlet of the perpendicular channel. The two PMMA plates were sealed together by the thermal-pressing technique and the joints were sealed by epoxy adhesive. The micropipette was made from a glass capillary (ID 500 μm) with a micropipette puller (P-30, Sutter Instrument Co.), and its tip was cut in the range of 100–150 μm in inner diameter. The sodium alginate solution used as the continuous phase was obtained by dissolving 0.75 g of sodium alginate powder and 0.15 g of SDS in 50 g of deionized water under a magnetic stirring at room temperature for 2 h. An oil phase, typically liquid paraffin, was used as the dispersed phase. In some cases, small amount of sudan III was added in liquid paraffin to facilitate the observation of the dispersed phase. A 10 wt % $CaCl_2$ solution was prepared for the reaction with sodium alginate solution to get the calcium alginate fiber. During the preparation, the alginate solution was introduced in device through the perpendicular channel by one syringe pump, while the liquid paraffin was injected through the metal needle by another syringe pump (PHD 2000 Syringe, Harvard). The core flow rate was fixed at 25 μm min^{-1} and the dispersed phase flow rate varied between 2.5 to 15 μm min^{-1}. The outlet of the micropipette was immersed vertically into the $CaCl_2$ solution. All measurements and observations were conducted after residing in the $CaCl_2$ solution for more than 30 min to complete gelation of the calcium alginate. A high-speed camera was used to acquire images of the flow patterns in the micropipette and the formation of the alginate fiber in the $CaCl_2$ solution. A schematic diagram of the experimental process and the microfluidic device is presented in Fig. 1.

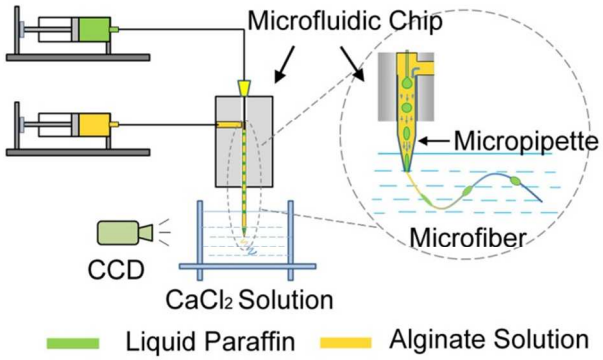

Fig. 1. Schematic diagram of the experimental process for preparation of the fibers with spindle-knots.

Experiments on the water-collecting ability of the fiber with spindle-knots. The water collecting ability of the alginate fiber was measured by placing it horizontally on a U-shape sample holder in a PMMA chamber. A Spray gun was used to spray water into the chamber for 15 min. The U-shape sample holder hanging with the fiber was taken out and put under an optical microscopy for observation afterward. The volume of water drop on the fiber was calculated by the equation of $V=4\pi r_a^2 r_b/3$.[18] Where, r_a and r_b are the horizontal radius and vertical radius of a water drop, respectively.

Characterization of calcium alginate fibers. Microdroplets were observed by a high-speed CCD camera (MVC610DAM/C-GE110, MicroView) and microfibers were observed by an optical microscope (CX31, Olympus). Water drops hanging on the fibers were observed and analysed by both of the optical microscope and CCD camera.

Results and Discussion

Fabrication of calcium alginate fibers

We first conducted the experiments in the microfluidic device with a glass capillary (ID 500 μm) at the continuous phase and dispersed phase flow rates of 25 and 15 μL·min^{-1}, respectively. We observed the flow patterns in and at the outlet of the capillary through a high-speed camera. The obtained picture (Fig. 2a) shows formation of bullet-shaped liquid paraffin microdroplets with diameters of about 345 μm and an interval of 500 μm. As the outlet of the capillary was immersed in the $CaCl_2$ solution, the effluent was quickly solidified, forming a transparent fiber. Observation of a piece of fiber which was taken out of the $CaCl_2$ solution right after its formation by optical microscope (Fig. 2b) reveals that the fiber is constructed

by a straight string with a diameter of 420 μm enwrapping with oval-shaped microdroplets. The enwrapped microdroplets are 330 μm in the longest diameter, 260 μm in the shortest diameter, and 290 μm in intervals. We also observed that the fiber shrank obviously after about 30 min during the observation, resulting in a decrease in its diameter to 300 μm (Fig. 2c). This is caused by dehydration of the calcium alginate fiber.

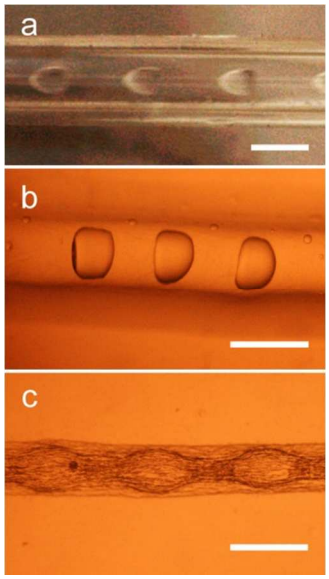

Fig. 2. (a) Image of liquid paraffin microdroplets in the glass capillary. (b) Image of calcium alginate fibers taken out right after its formation. (c) Image of calcium alginate fibers after being left in the air for 30 min. The scale bar is 500 μm.

We later pulled the glass capillary (ID 500 μm) with a micropipette puller to a micropipette with inner diameter of 150 μm, and replaced the capillary with this micropipette. Preparation of the fiber was conducted at the oil phase flow rate of 10 μL·min^{-1}. The obtained microdroplets are 267 μm in diameter, smaller than those obtained using the glass capillary (ID 500 μm). When the microdroplets flowed in the constricted section, they transformed from bullet shape to ellipsoidal shape. Immediately after they flowed out of the micropipette, these ellipsoidal microdroplets tried to change back to their previous equilibrium shape. At the same time, a transparent fiber was jetted continuously from the outlet of the micropipette, in which the microdroplets were enwrapped. Optical microscopic observation of the just-prepared fiber reveals spindle-knots on it (Fig. 3a). The diameter of the fiber between every two adjacent knots is ca. 90 μm. These knots show ellipsoidal morphology, with a height of 200 μm, a width of 480 μm and interval of 1900 μm. The fiber shrank obviously after being left on the objective table of the optical microscope for 30 min, evidenced by decrease in the diameter of the fiber to 64 μm (Fig. 3b). However, the sizes of the knots do not change significantly, with a slight decrease in the height to 190 μm and an increase in the width to 515 μm. Therefore, we can prepare calcium alginate fibers with spindle-knots structure by a simple microfluidic technique. The formation process can be described as flow of the liquid paraffin microdroplets with the sodium alginate solution in the straight microchannel, constriction of both the microdroplets and the sodium alginate solution at the outlet of the micropipette, fast gelation of the constricted sodium alginate solution and recovery of the constricted microdroplets at the same time once they flow out of the micropipette, and shrinkage of the fiber because of dehydration.

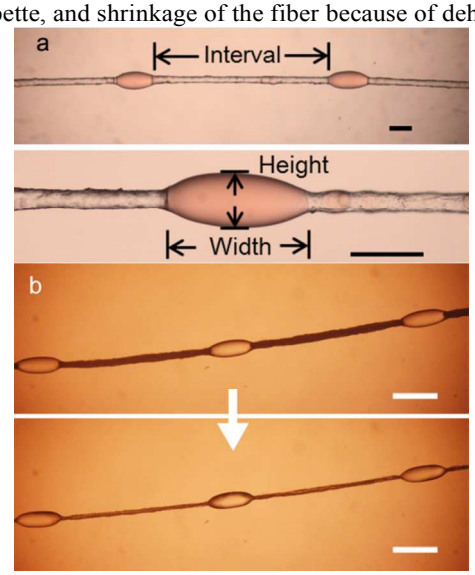

Fig. 3. (a) Image of calcium alginate fiber with spindle-knots taken out right after its formation. (b) Image of the calcium alginate fiber shrank process after being left in the air for 30 min. The scale bars are (a) 250 μm and (b) 500 μm.

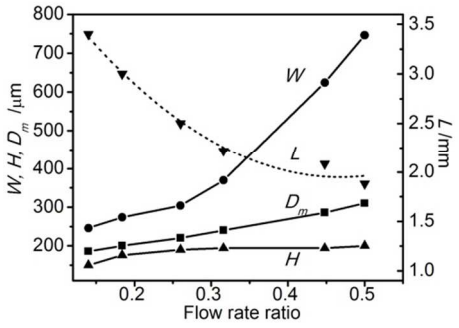

Fig. 4. Effect of dispersed phase flow rate on the height (*H*) and width (*W*) of the knot, the diameter of the resultant microdroplet in the capillary (D_m) and the interval between two adjacent knots (*L*). The relationship via fitting of data of *L* is drawn as the red line.

Effect of two-phase flow rate ratio

As the dispersed phase to the continuous phase flow rate ratio can significantly influence the diameter of the microdroplets,[19] we examined its effect on the structure and size of the fiber with spindle-knots. Fig. 4 shows the diameter of the resultant microdroplet, the height and width of the knot as a function of the flow rate ratio by keeping the continuous phase flow rate at 25 μL·min^{-1}. With increasing the flow rate ratio, the diameter of the microdroplets increases linearly from 180 to 310 μm and this trend is the same as those reported in literature.[20] The width of the knot increases slowly from 246 to 304 μm as increasing the flow rate ratio from 0.125 to 0.25, and increases dramatically to 746 μm with further increase in the flow rate

ratio to 0.5, demonstrating the significant influence of the flow rate ratio on the width of the knot when it is higher than 0.5. However, the height of the knot increases from 150 to ca. 190 μm as increasing the flow rate ratio from 0.125 to 0.25. Further increase in the flow rate ratio to 0.5 leads to slightly increase in the height of the knot to 194 μm, indicating that the flow rate ratio does not exert obvious influence on the height of the knot when it is higher than 0.5.The interval between the two adjacent knots decreases from about 3.4 to 1.9 mm as the flow rate ratio increases.

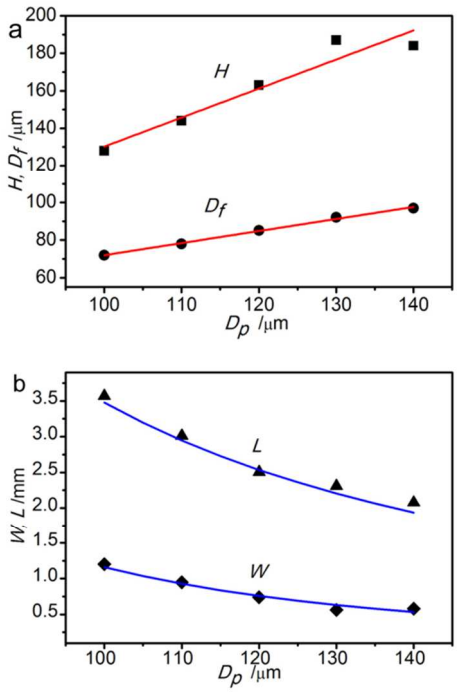

Fig. 5. (a) Effect of the micropipette diameter (D_p) on the height (H) of the knot and the diameter (D_f) of fiber. (b) Effect of the micropipette outlet diameter (D_p) on the width (W) and interval (L) of the knot. The lines in (a) and (b) are, respectively, the fitting lines of data and prediction lines from the deduced equations.

Effect of the micropipette diameter

We examined the effect of the micropipette diameter as it may determine the structure of the knot. Fig. 5 shows the diameter (D_f) of the fiber (that is calculated after taking out right after its formation), the width (W), height (H) and interval (L) of the knot as a function of the micropipette diameter. We fixed the dispersed phase flow rate of 10 μL·min^{-1} and the flow rate ratio as 0.4. Under such an experimental condition, the microdroplet diameter is 280 μm. Obviously, both of H and D_f increase linearly from 128 to 184 μm and 72 to 97 μm (Fig. 5a), and W and L decrease from 1.2 to 0.58 mm and 3.8 to 2 mm with increasing the micropipette diameter (Fig. 5b). The relationships of H and D_f to the microdroplet diameter can be expressed as H=1.55 D_p-24.8, D_f=0.64 D_p+8 by fitting the data using the least square fitting method. From the two equations and by assuming the knots as ellipsoids and the fiber as cylinder, we can predict the relationships of W and L to the microdroplet diameter D_p based on the volume conservation with equations: $W = D_m^3/H^2$ and $L= V_a /\pi (D_f/2)^2$. Where, V_a is the volume of alginate solution between two adjacent microdroplets. We plotted the prediction results also in Fig. 5b, which shows consistency to the experimental results. Based on these data, assumption that the knots are ellipsoids, and the constant volume of the oil microdroplet before and after the deformation, we can estimate the thickness of the calcium alginate layer covering on the knots by first obtaining the height of the deformed oil droplet ($H_{knot\text{-}oil}$), followed by dividing the difference between the height of the knot (H) and $H_{knot\text{-}oil}$ with 2. The result shows that the thickness is less than 2 μm.

The above results indicate that both flow rate ratio and micropipette diameter can affect the structure of the knots. To examine which factor has more strong influence on either the width or height of the knots, we analyzed the data by using the orthogonal array test to obtain the statistical significance of the two factors. Two-Way ANOVA in OriginPro 8.0 was used and the results demonstrate that the corresponding pre-specified low probability threshold values (p-value) are less than 0.01, indicating that both the flow rate ratio and micropipette diameter are statistically significant. Therefore, we can easily adjust the dimension of the knots by simply changing the flow rate ratio or the micropipette diameter.

3.4 Physical properties of dispersed phase fluid

To investigate if this structured calcium alginate fiber can be formed with the oil phases other than liquid paraffin as the dispersed phase, we chose 10 organics of which the physical properties in the interfacial tension, the density or the viscosity are close to one of those of the liquid paraffin. The micropipette with a diameter of 150 μm was used and the dispersed phase to the continuous phase flow rate ratio was fixed as 0.5. We found that uniform microdroplets can be formed by any oil phase. The fiber was immediately formed at the outlet of the micropipette, as in the case of using liquid paraffin as the oil phase. At the same time, the microdroplets flowed out of the micropipette with the sodium alginate solution. They were either enwrapped in the fiber forming the knots, or escaped from the fiber, or partly enwrapped and partly escaped, depending on the organics used. We summarized these results according to the interfacial tension, the density, and the viscosity in Fig. 6. In terms of the interfacial tension (Fig. 6a) and the density (Fig. 6b), the fiber with knots can be formed at medium values of 8-16 mN·m^{-1} and 0.8-1.0 g·mL^{-1}, although the formation is not definite. In terms of the viscosity, it is very distinct that the microdroplets escaped from the fiber when using the organics with viscosity of lower than 8 cP (Fig. 6c), and they can be enwrapped in the fiber when using the organics with the viscosity of higher than 40 cP. This correlation between the viscosity of the oil phase and the formation of the fiber with knots indicates the significance of the viscosity. This can be explained by more microdroplet orientation towards the flow direction for the lower viscosity ratio and less orientation towards the flow direction for the higher viscosity ratio.[21,22] This means that the microdroplets containing the organics with

a lower viscosity tend to escape from the continuous phase during deflection of the formed alginate fiber in the $CaCl_2$ bath. The density and interfacial tension, respectively, have influence on the gravity and the characteristic time for microdroplet shape relaxation. The gravitational forces can be neglected most of the time in the microfluidic system.[23] Hence, the gravitational effect is sufficiently small and the density has negligible influence on the formation of the structured fiber. The interfacial tension determines the characteristic time for microdroplet shape relaxation, which is less than 0.022 s in this case (estimated by the equations at uniform flow velocity mentioned in the literature[16]), much less than the gelation time of calcium alginate (ca. 0.27 s, estimated by the equations at 10 wt% $CaCl_2$ mentioned in the literature[24].) . Therefore, the deformed microdroplets, right after flowing out of the micropipette, are mainly recovered to the spherical shape before they are enwrapped by calcium alginate. They tended to escape from the alginate fluid when other physical properties of the organics did not influence the flow status of microdroplets in alginate fluid.

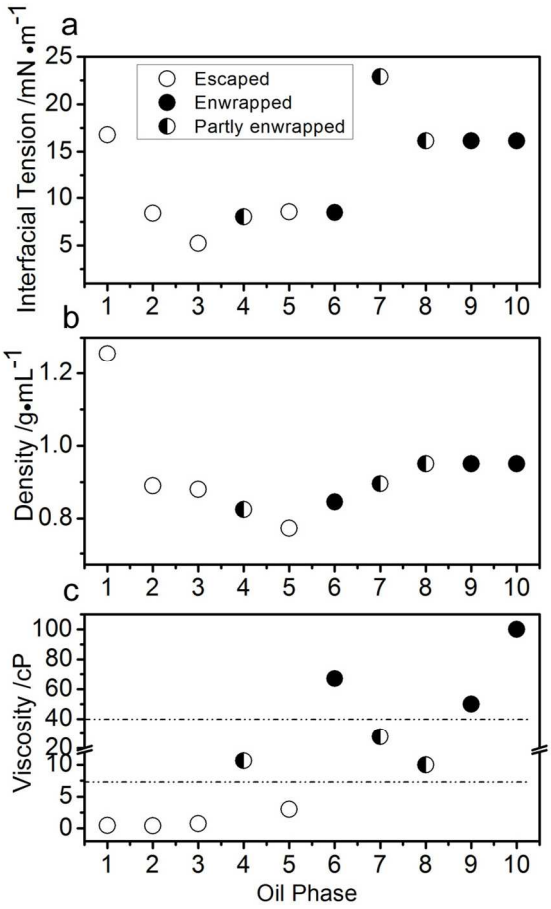

Fig. 6. Effect of various oil phases on the encapsulation and escapement of the oil phase microdroplets in the calcium alginate fibers: (a) the effect of the interfacial tension; (b) the effect of the density; (c) the effect of the viscosity of the oil phase. 1) 1,2-dichloroethane; 2) n-heptane; 3) o-xylene; 4) 1-octanol; 5) n-hexadecane; 6) liquid paraffin; 7) oleic acid; 8) dimethylsilicone oil DC-200/10; 9) dimethylsilicone oil DC-200/50; 10) dimethylsilicone oil DC-200/100.

Water collection behavior

The fibers with spindle-knots are known for the ability to mimic the water collecting behavior of spider silk. We thus examined the water collecting capabilities of the alginate fibers. Fig. 7a, b and c show the optical microscopic image of the fiber taken perpendicularly (Fig. 7a, b) and horizontally (Fig. 7c) after the water collecting experiment. Obviously, water drops can be formed on both the fiber and the knots (Fig. 7a, c). However, Fig. 7c shows that the water drop hanging on the knot (V=2.07 μL) is much larger than that on the fiber (V= 0.31 μL). We obtained the relationship of the volume of hanging water drop to the width of the knot, which can be expressed as $V = 2.64W - 0.26$, as illustrated in Fig. 7d. Therefore, the water collecting capability of the fiber depends on the width of the spindle-knot. These results are consistent with those on other fibers with similar structures,[24,25] which can be explained by continuous gradients of Laplace pressures which are generated from lower curvature on the knots.[26]The fibers are strong enough in normal handling and before and after the water collecting experiments. We also calculated the maximum tensile stress and the tensile strain at break according to the reference[27], which are 0.4677 MPa and 0.8962, respectively.

It is needed to be noted that knots on the fiber reported in this context are formed by encapsulation of oil phase microdroplets in calcium alginate fiber. Besides, the calcium alginate layer on the oil phase microdroplets is quite thin (less than 2 μm). This is advantageous for filtration of small amount of materials, such as bacteria or viruses,[28-30] in the air which are captured by water droplets toward the knots. Since there are full of organic liquid in the knots, it is possible to detect the captured and filtrated materials in the knots. Therefore, the calcium alginate fibers with spindle-knots may be used to detect bacteria or viruses in the air.

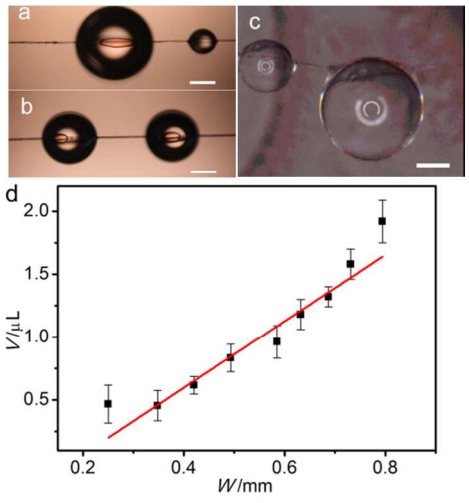

Fig. 7. Optical images of water drops on spindle-knots with different widths from the perpendicular direction: (a) width of the knot is ca. 730 μm; (b) width of the knot is ca. 350 μm. (c) Optical images of water drops on the knot observed from the horizontal direction. The width of knot is ca. 800 μm. The white circle on the drops is created by light from the camera; (d) Relationship of the volume (V) of the hanging water drop and the width (W) of knots. The scale bar is 500 μm.

Conclusions

We have demonstrated a new method to fabricate alginate fibers with spindle-knots, using a simple co-axial type microfluidic device with installation of a micropipette at its outlet. The deformation and retraction process of the microdroplets at the constriction part of the micropipette results in formation of the spindle-knots. The height, width, interval of the spindle-knots and the diameter of the fibers can be conveniently regulated by changing the two-phase flow rate ratio and the micropipette diameter. The viscosity of oil phase fluid is crucial for encapsulation or escapement of microdroplets, which determines the successful formation of the fibers with spindle-knots. These calcium alginate fibers also exhibit wettability, with dependence of the water-collecting capability on the width of the spindle-knot. As the alginate layer on the spindle-knots is very thin, it would be easy for the foreign objects in water droplets collected by the knots to diffuse into the oil phase microdroplets. Therefore, the method developed in this paper opens the possibility to simply fabricate functional materials, and the resultant fibers with spindle-knots may have potential application in the field of water collecting, biosensors and detection of bacteria or virus.

Acknowledgements

This work is supported by Natural Science Key Project of the Jiangsu Higher Education Institutions (12KJA530002), the Priority Academic Program Development of Jiangsu Higher Education Institutions.

Notes and references

[a] State Key Laboratory of Materials-Oriented Chemical Engineering, College of Chemistry and Chemical Engineering, No. 5 Xin Mofan Rd., Nanjing Tech University, Nanjing 210009, P. R. China.
[b] College of Mechanical and Power Engineering, No. 5 Xin Mofan Rd., Nanjing Tech University, Nanjing 210009, P. R. China.

1 G. T. Franzesi, B. Ni, Y. B. Ling and A. Khademhosseini, *J. Am. Chem. Soc.*, 2006, **128**, 15064.
2 J. J. Shi, A. R. Votruba, O. C. Farokhzad and R. Langer, *Nano. Lett.*, 2010, **10**, 3223.
3 R. J. Daher, N. O. Chahine, A. S. Greenberg, N. A. Sgaglione and D. A. Grande, *Nat. Rev. Rheumatol.*, 2009, **5**, 599.
4 J. W. Hong, V. Studer, G. Hang, W. F. Anderson and S. R. Quake, *Nat. Biotechnol.*, 2004, **22**, 435.
5 a) I. Yoo, S. Song, B. Yoon, J. M. Kim, *Macromol. Rapid Commun*. 2012, **33**, 1256; b) B. R. Lee, K. H. Lee, E. Kang, D. S. Kim and S. H. Lee, *Biomicrofluidics*, 2011, **5**, 22208; c) Y. Jun, M. J. Kim, Y. H. Hwang, E. A. Jeon, A. R. Kang, S. H. Lee and D. Y. Lee, *Biomaterials*, 2013, **34**, 8122.
6 a) A. L. Thangawng, P. B. Howell Jr, C. M. Spillmann, J. Naciri, F. S. Ligler, *Lab Chip*, 2011, **11**, 1157; b) D. A. Boyd, A. R. Shields, P. B. Howell and F. S. Ligler, *Lab Chip*, 2013, **13**, 3105–3110.
7 a)E. Kang, Y. Y. Choi, S. K. Chae, J. H. Moon, J. Y. Chang, S. H. Lee, *Adv. Mater.,* 2012, **24**, 4271; b) S. K. Chae, E. Kang, A. Khademhosseini and S. H. Lee, *Adv. Mater.*, 2013, **25**, 3071–3078; c) L. Leng, A. McAllister, B. Zhang, M. Radisic and A. Gunther, *Adv. Mater.*, 2012, **24**, 3650–3658.
8 a)C. H. Choi, H. Yi, S. Hwang, D. A. Weitz, C. S. Lee, *Lab Chip*, 2011, **11**, 1477; b) M. Yamada, S. Sugaya, Y. Naganuma and M. Seki, *Soft Matter*, 2012, **8**, 3122.
9 Y. M. Zheng, H. Bai, Z. B. Huang, X. L. Tian, F. Q. Nie, Y. Zhao, J. Zhai and L. Jiang, *Nature*, 2010, **463**, 640.
10 H. Bai, J. Ju, Y. M. Zheng and L. Jiang, *Adv. Mater.*, 2012, **24**, 2786.
11 H. Bai, X. L. Tian, Y. M. Zheng, J. Ju, Y. Zhao, L. Jiang, *Adv. Mater.*, 2010, **22**, 5521.
12 H. Bai, R. Z. Sun, J. Ju, X. Yao, Y. M. Zheng and L. Jiang, *Small*, 2011, **7**, 3429.
13 X. L. Tian, H. Bai, Y. M. Zheng and L. Jiang, *Adv. Funct. Mater.*, 2011, **21**, 1398.
14 L. Rayleigh, *Proc. London Math. Soc.*, 1878, **10**, 4.
15 E. Kang, G. S. Jeong, Y. Y. Choi, K. H. Lee, A. Khademhosseini and S. -H. Lee. *Nat. Mater.*, 2011, **10**, 877.
16 J. T. Cabral and S. D. Hudson, *Lab Chip*, 2003, **6**, 427.
17 S. D. Hudson, J. T. Cabral, W. J. Goodrum, Jr, K. L. Beers and E. J. Amis, *Appl. Phys. Lett.*, 2005, **87**, 081905.
18 Y. P. Hou, Y. Chen, Y. Xue, Y. M. Zheng and L, Jiang. *Langmuir*, 2012, **28**, 4737.
19 J. K. Nunes, S. S. H. Tsai, J. Wan and H. A. Stone, *J. Phys. D: Appl. Phys.*, 2013, **46**, 114002.
20 T. Cubaud and T. G. Mason, *Phys. Fluids.*, 2008, 20, 053302.
21 A. Vananroye, P. Van Puyvelde and P. Moldenaers, *J. Rheol.*, 2007, **51**,139.
22 P. L. Maffettone and M. Minale, *J. Non-Newtonian Fluid Mech.*, 1998, **78**, 227.
23 J. Berthier and K. A. Brakke, *The Physics of Microdroplets*, Wiley, 2012, pp. 168.
24 A. Blandino, M. Macias and D. Cantero, *J. Biosci. Bioeng.*, 1999, **88**, 686.
25 J. H. Xu, S. W. Li, J. Tan, Y. J. Wang and G. S. Luo, *Langmuir*, 2006, **22**, 7943.
26 E. Lorenceau and D. Quere, *J. Fluid Mech.*, 2004, **510**, 29.
27 T. R. Cuadros, O. Skurtys, J. M. Aguilera. *Carbohyd. Polym.*, 2012, **89**, 1198-1206.
28 Y. Bashan, *Appl. Environ. Microbiol.*, 1986, **511**, 1089.
29 A. S. Brady-Estevez, M. H. Schnoor, C. D. Vecitis, N. B. Saleh and M. Elimelech, *Langmuir*, 2010, **26**, 14975.
30 C. A. Axtell and G. A. Beattie, *Appl. Environ. Microbiol.*, 2002, **68**, 4604.

